

General Disclaimer

One or more of the Following Statements may affect this Document

- This document has been reproduced from the best copy furnished by the organizational source. It is being released in the interest of making available as much information as possible.
- This document may contain data, which exceeds the sheet parameters. It was furnished in this condition by the organizational source and is the best copy available.
- This document may contain tone-on-tone or color graphs, charts and/or pictures, which have been reproduced in black and white.
- This document is paginated as submitted by the original source.
- Portions of this document are not fully legible due to the historical nature of some of the material. However, it is the best reproduction available from the original submission.

NASA CONTRACTOR REPORT 166414

(NASA-CR-166414) QUANTUM CHEMICAL
CALCULATIONS FOR POLYMERS AND ORGANIC
COMPOUNDS (Surface Analytic Research, Inc.)
51 p HC A04/MF A01 CSCL 11C

N82-33528

G3/27 Unclass
35194

Quantum Chemical Calculations for Polymers and
Organic Compounds

J. Lopez
C. Yang



CONTRACT NAS2-10789

NASA

NASA CONTRACTOR REPORT 166414

**Quantum Chemical Calculations for Polymers and
Organic Compounds**

**J. Lopez
C. Yang
Surface Analytic Research, Inc.
Mountain View, California**

**Prepared for:
Ames Research Center**



**National Aeronautics and
Space Administration**

**Ames Research Center
Moffett Field, California 94035**

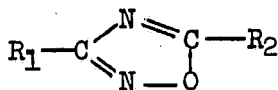
TECHNICAL OBJECTIVES

I. Quantum Calculations of Fluoroether Polymers

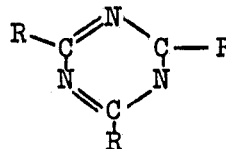
The overall purpose of this research was to help understand polyfluoroether chemistry with a combination of experimental results and quantum mechanical calculations. Thus, we have worked in close collaboration with Dr. Rosser at NASA-Ames Research Center who contributed to the experimental counterpart of this research. The interpretation of the experimental results obtained by Rosser and coworkers about the relative thermal and hydrolytic stability of perfluoroalkylether substituted 1,2,4-oxadiazole^{1,2} and 1,3,5-triazine² model compounds was the initial motivation of this investigation.

The two general systems that we have considered are shown in figure 1. The perfluoro and perfluoroether substituents used in the experimental model compounds contain as many as seven carbon atoms. For the case of 1,2,4-oxadiazole, a model compound where R₁ was a phenyl group bridging two 1,2,4-oxadiazole moieties has been synthesized and it has been found that its thermal stability decreases with respect to completed perfluorinated derivatives. For the case of 1,3,5-triazine^{it} was found that a branch (namely, a CH₃ group) at the carbon attached to the ring produced an extremely stable compound at high temperatures in different environments. Moreover, an unbranched perfluoro substituent was completely hydrolyzed by water at 325C.

Figure 1



(a) 1,2,4-oxadiazole derivatives



(b) 1,3,5-triazine derivatives

The theoretical aspect of this investigation was mainly a study of the effect that different substitution produces on the electronic structure of the heterocycle. Changes in geometry, atomic charge populations, and molecular orbital energies were extensively examined. Substituents of smaller size than those present in the experimental model compounds have been used in the calculations. These substituents simulated the general characteristics of the real ones, and have the advantage of reduced computational effort.

II. Quantum Chemical Calculations for a One-dimensional Conductor

Another application of state-of-the-art quantum chemical methods under this contract was to a class of one-dimensional conductors. This class of conductors, of which $K_2Pt(CN)_4Br_{0.3} \cdot xH_2O$ (KCP) is one, has a chain structure consisting of staggered square planar tetracyanoplatinate complexes⁹.

Different complexes can be formed with varying concentrations of halogens which modify the oxidation states of Pt from +2.0 to as high as +2.4. Examples of these complexes are given in Table I. A schematic diagram of the tetracyanoplatinate chain is shown in Fig. 2. For metallic conduction, the top valence band of these complexes must be partially occupied. Since the bonding along the chain is through d_{z^2} electrons, this implies that partial oxidation depletes electrons from the d_{z^2} band. Prediction of partial oxidation from specific orbitals requires an accurate knowledge of the electronic structure. The objective of this research is to provide this knowledge of the electronic structure for the tetracyanoplatinate ion and to establish the orbitals from which partial oxidation occurs. The behavior of electrons in these orbitals are then correlated with the different Pt-Pt separations and electrical conductivities¹⁰. A more fundamental understanding of the general trend of increase in conductivity resulting from increase

Table I

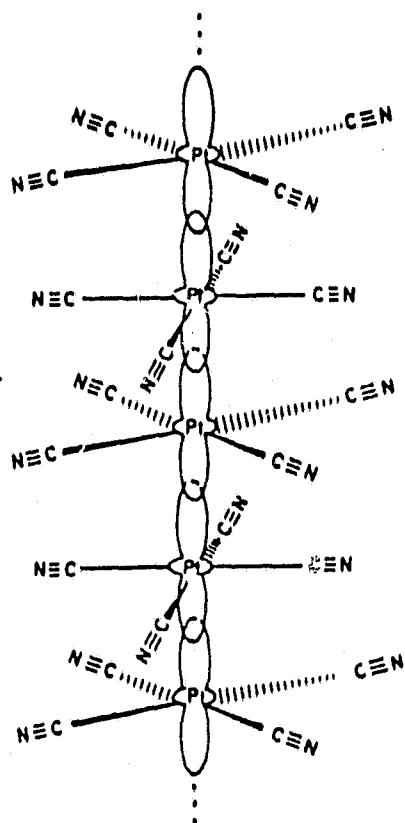
Some Tetracyanoplatinate Complexes *

<u>Complex</u>	<u>Pt-Pt (Å)</u>	<u>Conductivity $\Omega^{-1}\text{cm}^{-1}$</u>
Pt metal	2.775	10^5
$\text{K}_2\text{Pt}(\text{CN})_4$	3.50	10^{-7}
$\text{K}_2\text{Pt}(\text{CN})_4\text{Br}_{0.3}$	2.89	800
$\text{Cs}_2\text{Pt}(\text{CN})_4(\text{FHF})_{0.23}$	2.872	300
$\text{Cs}_2\text{Pt}(\text{CN})_4(\text{FHF})_{0.39}$	2.833	2000

* from Refs (9) & (10)

Figure 2

$[\text{Pt}(\text{CN})_4]_n^{2-}$ chain



in oxidation number for Pt coupled with decrease in Pt-Pt separation is sought.

RESEARCH ACCOMPLISHED

I. Quantum Calculations of Fluoroether Polymers

As a computational tool we started using the semiempirical MINDO/3 (Modified Intermediate Neglect of Differential Overlap) method of Dewar et al³.

(1) The s-triazine system

MINDO/3 calculations on the unsubstituted 1,3,5-triazine yielded a planar molecule. This result is in agreement with experimental data⁴. Then we started studying the effect of monosubstitution of CF_3CF_2 . The five fluorine atoms and the triazine ring were chosen to stay in a staggered conformation. Rotation of the triazine ring around the C-C bond was allowed, with the remaining geometrical parameters fixed. The goal of this calculation was to locate the neighborhood of the equilibrium conformation. The results of these calculations indicated that the most stable conformation was at a rotation angle of about 135 degrees. Consequently we started a calculation where we froze this angle and permit a partial relaxation of the geometry within the CF_3CF_2 group. The results obtained look very unrealistic: a large deviation of the C-C-C and F-C-C angles from the tetrahedral value brings the fluorine atoms to an excessive proximity.

Repetition of the calculation at 90° gave the same kind of anomalous result. We concluded that the cause of this problem resides in the underestimation of lone pair - lone pair electron repulsion between adjacent fluorine atom, in MINDO/3. Subsequently we decided to use the different quantum mechanical method MNDO⁵ (Modified Neglect of Diatomic Overlap) which has proved to be more accurate than MINDO/3 for molecules containing hetero-atoms.^{6,7}

MNDO calculations were then performed for unsubstituted s-triazine, and for monosubstitution of CF_3CF_2 . For the latter case the optimized geometry was much more realistic, and the heat of formation obtained was much less exothermic than that obtained with MINDO/3. For unsubstituted s-triazine, MINDO/3 and MNDO predicts practically the same geometry for the ring. This agreement would have been expected since the absence of fluorine atoms reduces the error coming from the underestimation of lone pair - lone pair electron repulsion.

MNDO calculations with the substituents $\text{CF}(\text{CF}_3)\text{CF}_3$ and $\text{CF}(\text{CF}_3)\text{OCF}_3$ were also performed. We successfully optimized all the geometrical parameters. No significant differences at the triazine ring are detected in geometries, charge distributions and molecular orbital diagrams for the three different substituents employed.

A close scrutiny of the molecular orbitals indicated that the loss of basicity of the triazine nitrogen atoms upon substitution is due to a drop of 0.8eV in the energy of the highest occupied molecular orbital of symmetry σ . Nevertheless differences in basicity between the three substituted s-triazine is not apparent. The differences in hydrolytic stability could be of thermodynamic and / or kinetic nature. Both possibilities are currently being examined.

(2) The 1,2,4-oxadiazole system

We started studying the 1,2,4-oxadiazole simultaneously with the s-triazine system. Consequently some MINDO/3 calculations were initially performed. MINDO/3 results for the unsubstituted heterocycle revealed that all the atoms of the ring lie in the same plane in agreement with experimental data⁸. A CF_3 group was substituted at carbon 3 (see figure 1a), and rotation of it around the C-C bond was allowed. The results indicated that: (a) a free

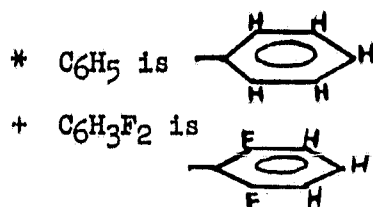
rotation of CF_3 is expected at room temperature, and (b) the rotation is practically rigid.

Due to the shortcomings of MINDO/3 as seen in the s-triazine calculations, we performed MNDO calculations on the unsubstituted 1,2,4-oxadiazole in order to see how the results differed from those of MINDO/3. The MNDO heat of formation was about 17 kcal/mol above the corresponding MINDO/3 value, suggesting that some underestimation of electronic repulsion might be present in the MINDO/3 calculation. Also the geometry was somehow different. Nevertheless a planar molecule was predicted in agreement with MINDO/3 result. With these results at hand, and recognizing the improvements of MNDO over MINDO/3 for system with heteroatoms^{6,7}, we decided to continue the study of this system with the MNDO method.

We have performed MNDO calculations for a series of molecules with different substituents R_1 and R_2 (figure 1(a)). Table II shows all the different cases considered. No details of all the different calculations are presented here. For this purpose the draft of a manuscript that we are preparing for publication is attached as an appendix. Here, only a summary of the conclusions achieved is given. Two important factors determine the thermal stability of the 1,2,4-oxadiazole structure: (a) the total negative charge inside the ring, and (b) the degree of homogeneity of such charge distribution. For phenylated derivatives, a non-planar conformation is the energetically most favored. Increasing the temperature would start populating the planar conformation, and as a result a greater number of electrons would be accumulated inside the oxadiazole ring, thus leading to reduced thermal stability. Stabilization of phenylated derivatives is suggested by avoiding the planar conformation as well as by the introduction of electron-withdrawing groups at ortho and para benzene ring positions.

Table II

R_1	R_2
H	H
CH ₃	H
CF ₃	H
C ₂ F ₅	H
CF ₃	CF ₃
C ₂ F ₅	CF ₃
C ₆ H ₅ *	H
C ₆ H ₅ .	CF ₃
C ₆ H ₃ F ₂ +	CF ₃
CF ₃	C ₆ H ₅



II. Quantum Chemical Calculations for a One-dimensional Conductor

The proposed calculations are performed using the self-consistent-field-X α -Dirac-Scattered-Wave (SCF-X α -DSW) method¹¹ for the clusters $[\text{Pt}(\text{CN})_4]^{-2}$ and $[\text{Pt}(\text{CN})_4]_3^{-6}$ for several Pt-Pt separations. This method has proven its utility in treating systems containing transition metals, and it treats relativistic effects exactly, which is vital to an accurate description of the Pt-Pt bond. The density of states is also calculated for each case. This study is intended as the first of a series of electronic structure calculations for one-dimensional conductors.

The monomer and trimer clusters each has D_{4h} point group symmetry. The density of occupied states for the monomer $[\text{Pt}(\text{CN})_4]^{-2}$ is shown in Fig. 3. The orbital with d_{z^2} character is in the middle of the Pt-ligand valence complex. This is to be expected since the monomer does not represent the extended chain system.

ORIGINAL PAGE IS
OF POOR QUALITY

Fig. 3 Density of occupied electronic states for $\text{Pt}(\text{CN})_4^{2-}$ based on the
SCF-X α -DSW molecular orbital energies

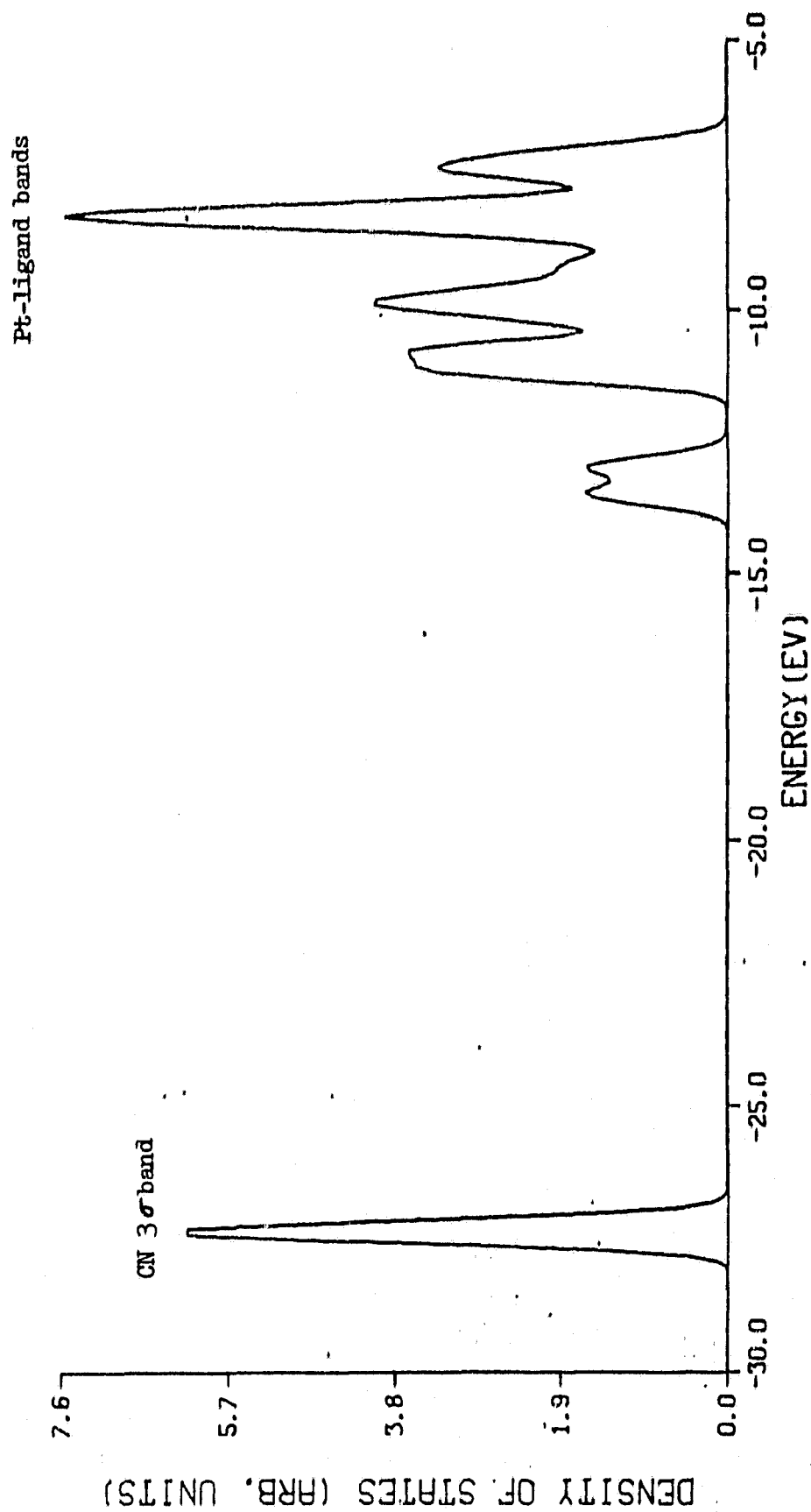
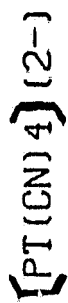
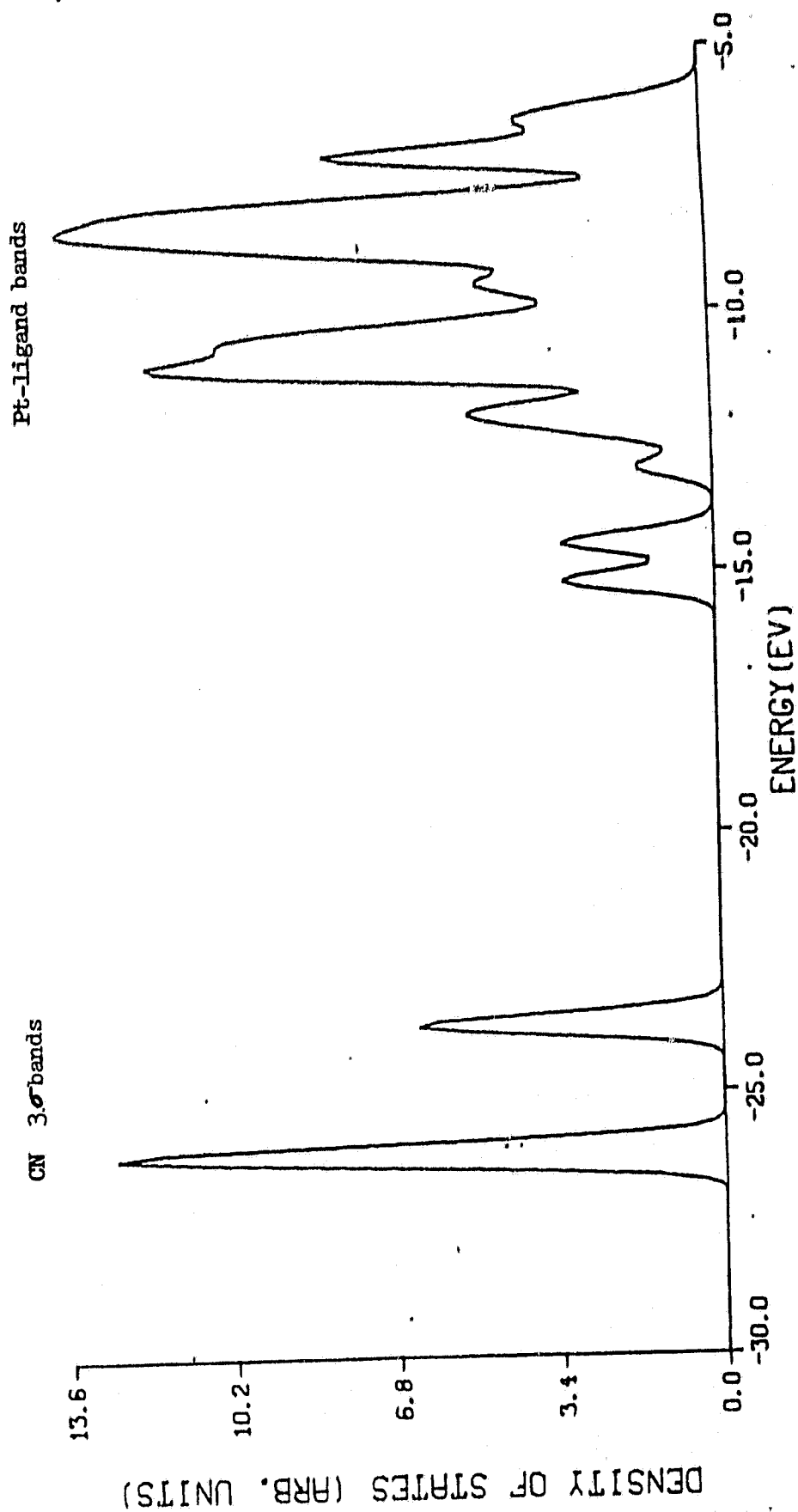


Fig. 4 Density of occupied electronic states for $[\text{Pt}(\text{CN})_4]^{2-}$ calculated from the SCF-X α -DSW molecular orbital energies



Substantial code developments have been made for the SCF-X α -DSW computer programs, so that it can handle the 27-atom trimer cluster $[\text{Pt}(\text{CN})_4]_3^{-6}$. The calculation for a Pt-Pt separation of 3.1Å has just been completed and the density of states is shown in Fig. 4. Preliminary analysis reveals that the antibonding d_{z^2} states are located at the top of the valence complex. However, the density of states near the valence band edge (E_v) is not exceedingly high. This is reasonable since the Pt-Pt separation used falls between those for the insulator and conductor compounds as seen in Table I. It is fair to speculate at this point that the density of states near E_v will be lower for large Pt-Pt separations (insulator) and much higher for smaller Pt-Pt separations (conductor). More detailed analysis of the trimer electronic structure as well as calculations for three other separations are ongoing.

PRESENTATIONS

MINDO/3 and MNDO calculations on Polyperfluoroalkyl Compounds, J.P. Lopez, C.Y. Yang and R. Rosser, The Third Annual West Coast Theoretical Chemistry Conference, Moffet Field, California, April 22-24, 1981.

REFERENCES

1. K.J.L. Paciorek, R.H. Kratzer, J. Kaufman, J.H. Nakahara, R.W. Rosser, and J.A. Parker, J. Fluorine Chem. 10, 119 (1977)
2. K.L. Paciorek, R.H. Kratzer, J. Kaufman, and R.W. Rosser, J. Fluorine Chem. 6, 241 (1975)
3. R.C. Bingham, M.J.S. Dewar, and D.H. Lo, J. Amer. Chem. Soc. 97, 1285 (1975)
4. P.J. Wheatley, Acta. Cryst. 8, 224 (1955)
5. M.J.S. Dewar and W. Thiel, J. Amer. Chem. Soc. 99, 4899 (1977)

6. M.J.S. Dewar and W. Thiel, J. Amer. Chem. Soc. 99, 4907, (1977)
7. M.J.S. Dewar and H.S. Rzepa, J. Amer. Chem. Soc. 100, 58 (1978)
8. L. Golic, I. Leban, B. Stanovnik, and M. Tislev, Acta Cryst. B35, 2256 (1979)
9. J.S. Miller and A.J. Epstein, Prog. Inorg. Chem 20, 1 (1976)
10. J.M. Williams, A.J. Schultz, K.B. Cornett, and R.E. Besinger, JACS 100, 5572 (1978)
11. C.Y. Yang and S. Rabi, Phys. Rev. A12, 362 (1975); C.Y. Yang, J. Chem. Phys. 68, 2626 (1978).

MNDO calculations

→ ~~Molecular Orbital Theory~~ Applied to Structural Changes In
1,2,4-Oxadiazole Substituents

INTRODUCTION

The literature describes the relative thermal stabilities of various substituted 1,2,4-oxadiazole compounds.^{1,2} General organic chemistry theory leaves many questions unanswered concerning the rationale of existing experimental data.

In this paper a theoretical study of the effect that the electron donor power of different substituents at positions 3 and 5 of the 1,2,4-oxadiazole ring has on the electronic structure of the heterocycle is undertaken. The results reported are all from the semi-empirical quantum mechanical Modified Neglect of Diatomic Overlap (MNDO) method³. This method has proven to be successful in the description of organic molecules containing heteroatoms⁴. We will discuss the results of Mulliken population analysis and a correlation molecular orbital diagram for a variety of selected molecules.

Figure I shows the general molecular system for which several calculations have been performed and, for simplicity, it is designated R_1 -OXA- R_2 in this paper. The objective of the work was to understand how the different substituents R_1 and R_2 modify the thermal stability of the 1,2,4-oxadiazole ring. We seek an answer to the question of how a particular substituent affects the electronic structure of the heterocycle, that is, does it favor dissociation of the ring or stabilize it.

Different combinations of the following substituents have been employed in the calculations: hydrogen, methyl, perfluoromethyl, perfluoroethyl, phenyl and

→ ~~o~~-bi-fluorophenyl.

2,6-difluorophenyl.

7 ~~The choice of~~ ^{were chosen} the substituents ~~have been motivated by the existence of~~ ^{from} similar experimental model compounds that are relevant to the synthesis of thermally stable polymeric materials. Particularly, Experiments have revealed that substitution of perfluoroalkyl groups on both carbon positions of the oxadiazole structure greatly stabilizes the ring system ^{1,2,5-trifluorophenyl}. The introduction of a phenyl group on the oxadiazole ring yields compounds which are not as stable as the completely perfluorinated derivatives ^{1,2,5}. ^{Regarding} ~~with respect to~~ ^{non-} the unfluorinated derivatives, it is known that the unsubstituted 1,2,4-oxadiazole is ~~very~~ ^{not} unstable. ^{hence} This stability is significantly enhanced by replacement of one of the hydrogens by a methyl group⁶.

Changes in atomic charge populations, geometries, and molecular orbital energies were extensively examined and in particular the effect of rotational conformers on the thermal stability of the phenyl substituted oxadiazoles will be discussed.

For ~~all~~ ^{the} calculations where the phenyl group was present, the geometry ~~of this group~~ ^{of the} was kept fixed at that of the free benzene molecule. A complete optimization of the ~~rest of the~~ ^{REMAINING} geometrical parameters was ^{then} performed. For the cases where the phenyl group ^{was} ~~is~~ absent, a complete optimization of the atomic arrangement was undertaken.

RESULTS

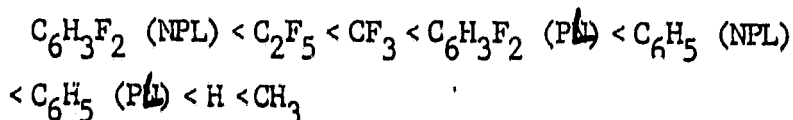
(a) Rotational Barriers

The calculations on all ~~the different molecules~~ ^{molecules} $R_1\text{-OXA-}R_2$ have shown that the five atoms of the oxadiazole ring lie in practically the same plane. Rotations around single bonds present insignificant barriers, except for the case of rotation of the phenyl group. Thus, the rotational barrier for $\text{CF}_3\text{-OXA-CF}_3$ is only 0.1 kcal/mol, whereas for $\text{C}_6\text{H}_5\text{-OXA-CF}_3$, $\text{C}_6\text{H}_5\text{-OXA-H}$, and $\text{CF}_3\text{-OXA-C}_6\text{H}_5$, they are 1.34, 1.28, and 1.16 kcal/mol respectively.

The potential energy curve for rotation of ^{the} phenyl group around the C-C single bond is depicted in Figure II for $C_6H_5-OXA-CF_3$. The two minima are at 64° and -64° away from the planar conformation. Since these ^{non-PLANAR (NPL)} ~~twisted~~ conformations are separated from the planar ^(PL) conformation by 1.34 kcal/mol, it is expected that at room temperature ^{non-PLANAR} ~~practically only~~ the ~~twisted~~ conformations are populated. ^{non planar} A quasi-free pass between the two ~~twisted~~ conformations must be expected because of the small barrier of separation between them (only 0.2 kcal/mol).

(b) Mulliken Population Analysis

Results within the 1,2,4-oxadiazole ring are presented in Table I. ^{An alternate} ~~A different~~ way to visualize the effect of substitution on the rearrangement of the atomic charge, is by examining the electron donor power of the substituents at positions 3 and 5 of the 1,2,4-oxadiazole ring. These results are shown in Table III. Inspection of the table reveals that the electron releasing power increases according to the following order:



The general ordering is in agreement with ^{what} ~~it~~ could be expected from qualitative arguments. It is interesting to observe the effectiveness of fluorine atoms in reducing the electron releasing power of the benzene structure. Also, it is seen that position 3 is a better ^{electron sink} ~~sink of electrons~~ than position 5, probably due to the ~~closest proximity~~ of the more electronegative oxygen atom (compared with nitrogen).

(c) Correlation Molecular Orbital Diagram

Diagram for seven of the molecules of Tables I and II is depicted in Figure III. In addition, and for reference purposes, the benzene molecule has also been included. The diagrams show the energies of only the highest double occupied molecular orbitals of each molecule. In principle, a molecular orbital is delocalized throughout the entire molecule; consequently, it should have contributions

from the oxadiazole ring as well as from the substituents. Nevertheless, an inspection of the highest occupied orbitals reveals that they are practically restricted to the oxadiazole and/or the benzene ring for all but one of the cases examined (the exception is $\text{CH}_3\text{-OXA-H}$). Molecular orbitals with significant contributions of the perfluoroalkyl substituents are much lower in energy. Since the 1,2,4-oxadiazole ring lies practically in the same plane for all the calculated structures, it is possible to classify the molecular orbitals that are "localized inside the ring" as of σ and π symmetry. This notation is used in Figure III for oxadiazole [π (o) and σ (o)] and for benzene [π (b) and σ (b)]. This notation is an approximate representation of the MO because of the 1,2,4-oxadiazole ring ~~is~~ ^{being} not perfectly planar, and because some tails from the perfluoroalkyl substituents are present in these orbitals. Moreover, the notation is useful because it shows the gross general character of the molecular orbitals.

The MO diagrams of C_6H_5 (NPL)-OXA- CF_3 and C_6H_5 (NPL)-OXA-H correspond to conformations where the oxadiazole is perpendicular to the benzene ring. The reasons why these conformations have been considered instead of the ~~most stable~~ ^{NPL configurations} ~~twisted ones~~ are due to: (i) an easier assignment of the character of the molecular orbital is performed, and (ii) the energies of the highest occupied MO are practically identical in both kinds of conformations.

(d) Geometry

A complete optimization of the geometry within the 1,2,4-oxadiazole ring was performed in all ~~the~~ cases. In general a very weak dependence of geometry upon substitution was found. As an illustration of the rearrangement of the atomic positions within the oxadiazole ring, the results of the equilibrium distances ~~are~~ ^{and} bond angles for four selected molecules are shown in Table III.

DISCUSSION

(A) Perfluoroalkyl Derivatives

Degradation studies have shown that 3,5-bis(perfluoro~~heptyl~~^{non-heptyl})-1,2,4-oxadiazole is thermally stable^{1, 2}. It remains undissociated for temperatures as high as 325°C in nitrogen and oxygen atmospheres; however, replacement of the perfluoro~~heptyl~~ substituent at position 3 by a phenyl group yields a structure which dissociates completely at 325°C.

Comparisons of the calculations for $\text{CF}_3\text{-OXA-CF}_3$, $\text{C}_2\text{F}_5\text{-OXA-CF}_3$ and $\text{C}_6\text{H}_5\text{-OXA-CF}_3$ help to rationalize the experimental results. For the phenylated derivatives there is an obvious relationship between the heating process and the distribution of conformational populations according to the results in Figure II. A rise in temperature increases the relative population of the Planar conformation; whereas low temperatures most of the molecules will exist in the nonplanar conformation^{or}. It is worth noting that at 325°C the thermal energy is of the same order of magnitude as the calculated rotational barriers between both extreme conformations; consequently, a significant increase in the population of the planar conformation is expected at this temperature. The immediate question that arises now is whether or not the existence of the planar conformation might ~~could~~ be responsible for the loss of stability of the 1,2,4-oxadiazole ring. Thus we need to see what properties of the heterocycle are modified in the transition from the non-planar to the planar structure, and then to see how these changes could eventually lead to a ring collapse. Changes in geometry, atomic charge population and molecular orbital diagram will be examined.

(i) Geometry: Even when the presence of the benzene ring, particularly in the planar conformation, produces the largest relative distortion in the oxadiazole ring, the changes are so small that it is difficult to know if they are related to ring rupture.

(ii) Atomic Charge Population: As can be seen from Table II, the planar conformation yields a greater accumulation of electrons inside the oxadiazole ring. This excess of negative charge could produce strain inside the ring leading to an eventual dissociation. On the other hand, the stable compounds $\text{CF}_3\text{-OXA-CF}_3$ and $\text{C}_2\text{F}_5\text{-OXA-CF}_3$ present the least accumulation of negative charge in the ring. In summary, the relative thermal instability of the phenylated derivatives seems to be due to the greater accumulation of electrons inside the 1,2,4-oxadiazole ring produced by population of the planar conformation at high temperatures.

(iii) Molecular Orbital Diagram: The ionization potentials obtained from Figure III, and assuming validity of Koopman's theorem, are: C_6H_5 (P) -OXA-CF_3 (9.92 eV), C_6H_5 (NPL) -OXA-CF_3 (9.99 eV), and $\text{CF}_3\text{-OXA-CF}_3$ (12.9 eV). The higher ionization potential of $\text{CF}_3\text{-OXA-CF}_3$ could explain the relative high oxidative stability of the completely perfluorinated derivatives. Introduction of benzene ring decreases the ionization potential, so the highest occupied MO's have electrons that are more readily transferable to an oxidizing agent. Inspection of MO diagram (Figure III) shows that the two highest occupied MO for the ~~studied~~^{NPL} conformation of $\text{C}_6\text{H}_5\text{-OXA-CF}_3$ are mainly localized in the benzene ring (at -9.99 and -10.10 eV). The next highest occupied MO belongs [?]practically to the oxadiazole ring with an eigenvalue of -11.77 eV. For the planar conformation, as ~~it could~~^{might} be expected, a delocalization of the electronic charges to both ring systems is found. Even when the IP does not change in a considerable amount, the character of the highest MO is altered. Now the HOMO (at -9.92 eV) has a significant contribution from the 2 p_z orbitals of the atoms located at the oxadiazole ring. For the planar conformation, the oxidation, ~~to~~^{to} some extent, involves removal of an electron from the oxadiazole. This would explain the decrease in oxidative thermal stability of the phenylated derivatives: The probability of oxidation of the oxadiazole ring increases with an increment of the temperature because the planar conformation has a greater population.

(B) Establishment of a More General Relationship

The number of electrons accumulated inside the 1,2,4-oxadiazole ring can be viewed as an "index" to predict differences in thermal stability. But, although this index explains the differences in stabilities between the completely fluorinated and the phenylated derivatives, ~~it fails within~~ ^{parts when} the stabilities of ~~CH₃-OXA-H and H-OXA-H are compared.~~ ^{CH₃-OXA-H is thermally more stable than H-OXA-H despite the fact that the oxadiazole ring has a greater negative charge for the former case (see Table II). Then a better index needs to be found. Such}

^{An improved} index should include (in addition to the total number of electrons released to the oxadiazole system) a measure of the charge distribution around the ring. It could be intuitive that an homogeneous distribution of a definite number of electrons will produce less strain in the ring than the same number of electrons but heterogeneously distributed. One way to have an indication of the homogeneity of the charge distribution is looking at the standard deviation of the charge. The results for the standard deviation and the new tentative index Ω are presented in Table IV. The index is defined as Ω = total number of electrons released to oxadiazole ring \times standard deviation. Thus ^a smaller value of Ω is associated with a more stable compound. A perfect correlation between Ω and those structures for which experimental information is available ^{was} found.

(C) Predictions of Thermal Stability

The index Ω can be used to predict the relative thermal stability of compounds for which experimental information is not available. The different values of Ω are shown in Table IV.

The thermal stability of the phenylated derivatives can be improved by decreasing the electron donor power of the benzene structure. This goal can be accomplished by attaching electron withdrawing groups to the benzene ring, and by avoiding the planar conformation. Both effects are nicely seen in $C_6H_3F_2-OXA-CF_3$ which is predicted to be ~~a~~ more stable structure (the smallest Ω). In this case,

a very ^{large} rotational barrier of 5.8 kcal/mol separates the non-planar (now at 78°) from the planar conformation. A temperature as high as 2630°C is needed in order to provide a thermal energy of 5.8 kcal/mol, thus the non-planar conformation is expected to have greater population.

Examination of MO diagram for $C_6H_3F_2$ -OXA- CF_3 reveals a general lowering of the energy levels compared with C_6H_5 -OXA- CF_3 . The ionization potential increases from 9.9 to 10.3 eV. In addition, the character of some of the highest occupied MO's is also modified. For the non-planar conformation the two highest occupied MO's are mainly of benzene character (at -10.27 and -10.80 eV); but the next highest MO (at -11.84 eV) has contributions from both rings in contrast to the equivalent MO of C_6H_5 (NPL)-OXA- CF_3 which is only localized in the oxadiazole ring. Although ^{for} the planar conformation of $C_6H_3F_2$ -OXA- CF_3 there is, as expected (see Figure III), a larger contribution of the oxadiazole ring in one of the highest occupied MO's, however, it is not expected that a significant population of this conformation for temperatures at 1000° or even 1500°C for example due to the high rotational barrier that separate it from the non-planar conformation. In summary, a greater inertness to removal of electrons from the oxadiazole ring must be expected by fluorination of benzene ring.

The value of the total charge released to the oxadiazole ring is about the same regardless if the phenyl group is attached to carbon 3 or carbon 5 as can be observed from Table IV for C_6H_5 -OXA- CF_3 and CF_3 -OXA- C_6H_5 respectively. But ^{the} phenyl group at position 5 generates a less homogeneous distribution of this charge as can be deduced from the values of the standard deviation shown in Table IV. Accordingly, substitution of ^a phenyl group at position 5 of ^{the} 1,2,4-oxadiazole predicts compounds thermally less stable.

(A) Consequently, a greater inertness to removal of electrons from the oxadiazole ring is expected for the non-planar conformation of $C_6H_3F_2$ -OXA- CF_3 . This relative inertness is partially lost for the planar conformation of $C_6H_3F_2$ -OXA- CF_3 because a larger contribution of the oxadiazole ring in one of the highest occupied MO's is observed. (This would be expected due to π delocalization to both rings - see Figure III). Accordingly, more electrons of the oxadiazole ring are now available for removal. Nevertheless, due to the huge rotational barrier, population of the planar conformation will be important only for very high temperatures (over $2000^\circ C$). In summary, the oxidative thermal stability of the oxadiazole ring is predicted to be improved by the presence of the 2-fluorine substituents on the phenyl ring.

ORIGINAL PAGE IS
OF POOR QUALITY

SUMMARY

The loss of stability of the 1,2,4-oxadiazole ring with various substituents is due to population of the less stable planar conformation at high temperatures, which by accumulation of excessive number of electrons inside the heterocycle could lead to dissociation. The thermal oxidation seems to be favored by π delocalization since some fraction of the electrons are now located in high energy levels of the 1,2,4-oxadiazole ring.

Recognizing that two important factors determining the stability of the 1,2,4-oxadiazole structure, ^{i.e.} the total negative charge inside the ring, and its corresponding distribution, a tentative index to predict thermal stability has been proposed.

Stabilization of the 1,2,4-oxadiazole ring for the cases of phenylated derivatives is suggested by avoiding the planar conformation as well as by the introduction of electron withdrawing groups ^{o and p} at benzene ring positions.
^

Bibliography

1. K. L. Paciorek, R. H. Kratzer, J. Kaufman, and R. W. Rosser: J. Fluorine Chem., 6, 241 (1975)
2. K. J. L. Paciorek, R. H. Kratzer, J. Kaufman, J. H. Nakahara, R. W. Rosser and J. A. Parker: J. Fluorine Chem., 10, 119 (1977)
3. M. J. S. Dewar and W. Thiel, J. Amer. Chem. Soc., 99, 4899 (1977)
4. M. J. S. Dewar and W. Thiel, J. Amer. Chem. Soc., 99, 4907 (1977); M. J. S. Dewar and H. S. Rzepa, ibid, 100, 58 (1978)
5. J. P. Critchley and J. S. Pippett, J. Fluorine Chem. 2, 137 (1972/73)
6. C. Mousseboid and J. F. M. Oth, Helvetica Chimica Acta 47, 942 (1964)

Handwritten notes and signatures:

✓ ~~CONFIDENTIAL~~

2. Surface Analysis

and (12) 12-12-22

NTSA - 11-11-11

TABLE I. Mulliken Population Analyses Within 1,2,4-Oxadiazole Ring. The charge on each atom is given in number of electrons. The numbering of the atoms is that given in Figure 1.

Molecule	O ₁	N ₂	C ₃	N ₄	C ₅	Total charge of 1,2,4- oxadiazole ring
H-OXA-H	-0.065	-0.111	+0.007	-0.249	+0.096	-0.322
CF ₃ -OXA-H	-0.047	-0.020	-0.098	-0.198	+0.109	-0.254
C ₂ F ₅ -OXA-H	-0.044	-0.016	-0.110	-0.192	+0.110	-0.252
CF ₃ -OXA-CF ₃	+0.002	+0.012	-0.098	-0.121	-0.002	-0.207
C ₂ F ₅ -OXA-CF ₃	+0.005	+0.017	-0.106	-0.120	-0.001	-0.205
C ₆ H ₅ (PL)-OXA-H*	-0.063	-0.113	+0.048	-0.245	+0.095	-0.278
C ₆ H ₅ (NPL)-OXA-H*	-0.067	-0.098	+0.041	-0.237	+0.093	-0.268
C ₆ H ₅ (PL)-OXA-CF ₃ *	-0.012	-0.085	+0.058	-0.170	-0.013	-0.222
C ₆ H ₅ (NPL)-OXA-CF ₃ *	-0.015	-0.068	+0.049	-0.158	-0.018	-0.210
CF ₃ -OXA-C ₆ H ₅ (PL)*	-0.048	-0.030	-0.094	-0.210	+0.161	-0.221
CF ₃ -OXA-C ₆ H ₅ (NPL)*	-0.040	-0.027	-0.100	-0.192	+0.154	-0.205
CH ₃ -OXA-H	-0.065	-0.100	-0.022	-0.239	+0.095	-0.332
C ₆ H ₃ F ₂ (NPL)-OXA-CF ₃ ,†	-0.009	-0.043	+0.037	-0.145	-0.012	-0.173
C ₆ H ₃ F ₂ (PL)-OXA-CF ₃	-0.007	-0.049	+0.033	-0.147	-0.017	-0.187

*PL and NPL refer to the planar and to the minimum energy non planar conformations respectively.

†C₆H₃F₂ is a phenyl group where the two hydrogen atoms of the benzene ring that are closest to the ^{ORTHO-}oxadiazole ring are substituted by fluorine atoms.

ORIGINAL PAGE IS
OF POOR QUALITY

TABLE II. Number of electrons released to the 1,2,4-oxadiazole ring by several substituents. For the sake of clarity, the substituent group is shown in the parenthesis next to the number.

Molecule	At C ₃	At C ₅	Total
H-OXA-H	0.153 (H)	0.169 (H)	0.322
CH ₃ -OXA-H	0.163 (CH ₃)	0.169 (H)	0.332
CF ₃ -OXA-H	0.072 (CF ₃)	0.182 (H)	0.254
C ₂ F ₅ -OXA-H	0.068 (C ₂ F ₅)	0.184 (H)	0.252
CF ₃ -OXA-CF ₃	0.090 (CF ₃)	0.117 (CF ₃)	0.207
C ₂ F ₅ -OXA-CF ₃	0.085 (C ₂ F ₅)	0.120 (CF ₃)	0.205
C ₆ H ₅ (Ph)-OXA-H	0.111 (C ₆ H ₅)	0.167 (H)	0.278
C ₆ H ₅ (NPL)-OXA-H	0.100 (C ₆ H ₅)	0.168 (H)	0.268
C ₆ H ₅ (Ph)-OXA-CF ₃	0.131 (C ₆ H ₅)	0.091 (CF ₃)	0.222
C ₆ H ₅ (NPL)-OXA-CF ₃	0.118 (C ₆ H ₅)	0.092 (CF ₃)	0.210
CF ₃ -OXA-C ₆ H ₅ (Ph)	0.065 (CF ₃)	0.156 (C ₆ H ₅)	0.221
CF ₃ -OXA-C ₆ H ₅ (NPL)	0.066 (CF ₃)	0.139 (C ₆ H ₅)	0.205
C ₆ H ₃ F ₂ (NPL)-OXA-CF ₃	0.077 (C ₆ H ₃ F ₂)	0.096 (CF ₃)	0.173
C ₆ H ₃ F ₂ (Ph)-OXA-CF ₃	0.092 (C ₆ H ₃ F ₂)	0.095 (CF ₃)	0.187

TABLE III. Equilibrium Geometry of 1,2,4-oxadiazole ring

(a) Interatomic Distances (Å)

Molecule	C ₃ -N ₄	N ₄ -C ₅	O ₁ -C ₅	O ₁ -N ₂	N ₂ -C ₃
H-OXA-H	1.4022	1.3352	1.3708	1.3003	1.3516
C ₂ F ₅ -OXA-CF ₃ ^a	1.4005	1.3344	1.3717	1.2895	1.3576
C ₆ H ₅ (NPL)-OXA-CF ₃	1.4080	1.3333	1.3695	1.2954	1.3579
C ₆ H ₅ (PX)-OXA-CF ₃	1.4106	1.3321	1.3684	1.2941	1.3608

(b) Bond Angles (Degrees)

Molecule	C-O-N	O-N-C	N-C-N	C-N-C	N-C-O
H-OXA-H	109.067	107.273	110.028	103.449	110.184
C ₂ F ₅ -OXA-CF ₃	109.138	107.340	109.960	103.203	110.353
C ₆ H ₅ (NPL)-OXA-CF ₃	108.667	107.844	109.413	103.270	110.805
C ₆ H ₅ (PX)-OXA-CF ₃	108.619	108.290	108.675	103.741	110.671

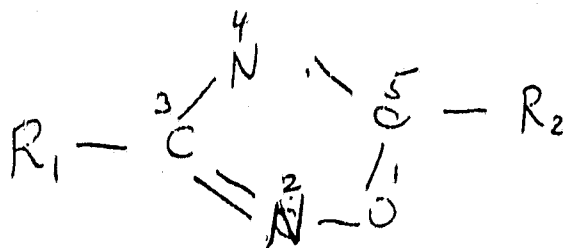
TABLE IV. Standard deviation of the atomic charge distribution inside the 1,2,4-oxadiazole ring

<u>Molecule</u>	<u>Standard Deviation</u>	<u>Total Charge of Oxadiazole Ring</u>	<u>Δ</u>
H-OXA-H	0.116	0.322	0.0374
CH ₃ -OXA-H	0.109	0.332	0.0362
CF ₃ -OXA-H	0.100	0.254	0.0254
C ₆ H ₅ (NPL)-OXA-H	0.115	0.268	0.0308
C ₆ H ₅ (PN)-OXA-H	0.121	0.278	0.0336
C ₆ H ₅ (NPL)-OXA-CF ₃	0.069	0.210	0.0145
C ₆ H ₅ (PN)-OXA-CF ₃	0.077	0.222	0.0171
CF ₃ -OXA-CF ₃	0.056	0.207	0.0116
CF ₃ -OXA-C ₆ H ₅ (NPL)	0.114	0.205	0.0234
CF ₃ -OXA-C ₆ H ₅ (PN)	0.120	0.221	0.0265
C ₆ H ₃ F ₂ (NPL)-OXA-CF ₃	0.061	0.173	0.0106
C ₆ H ₃ F ₂ (PN)-OXA-CF ₃	0.061	0.187	0.0114

ORIGINAL PAGE IS
OF POOR QUALITY

Figure I

3,5 - substituted 1,2,4 - oxadiazoles : R_1-OH



R_1 and R_2 are either of the following substituents:
 H , CF_3 , C_2F_5 and C_6H_5 (phenyl).

ORIGINAL PAGE IS
OF POOR QUALITY

ORIGINAL PAGE IS
OF POOR QUALITY

Fig. II

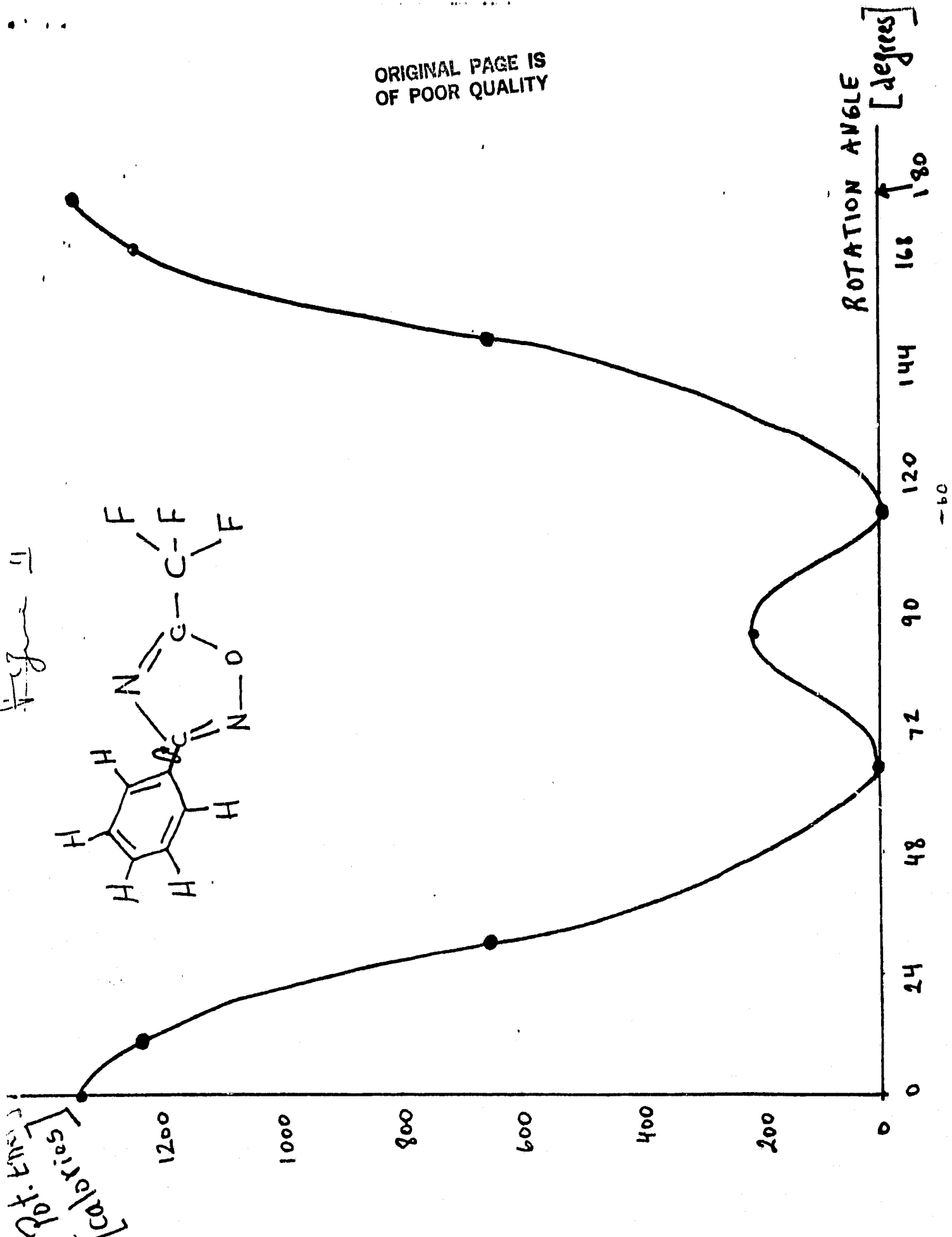
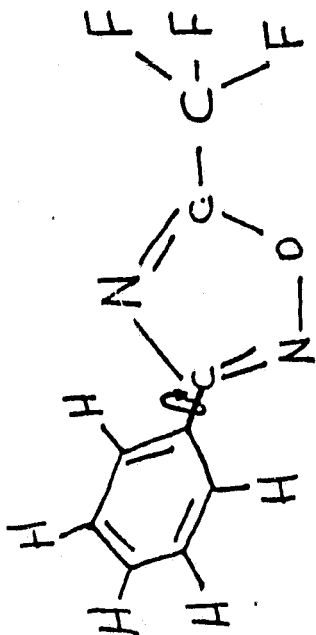
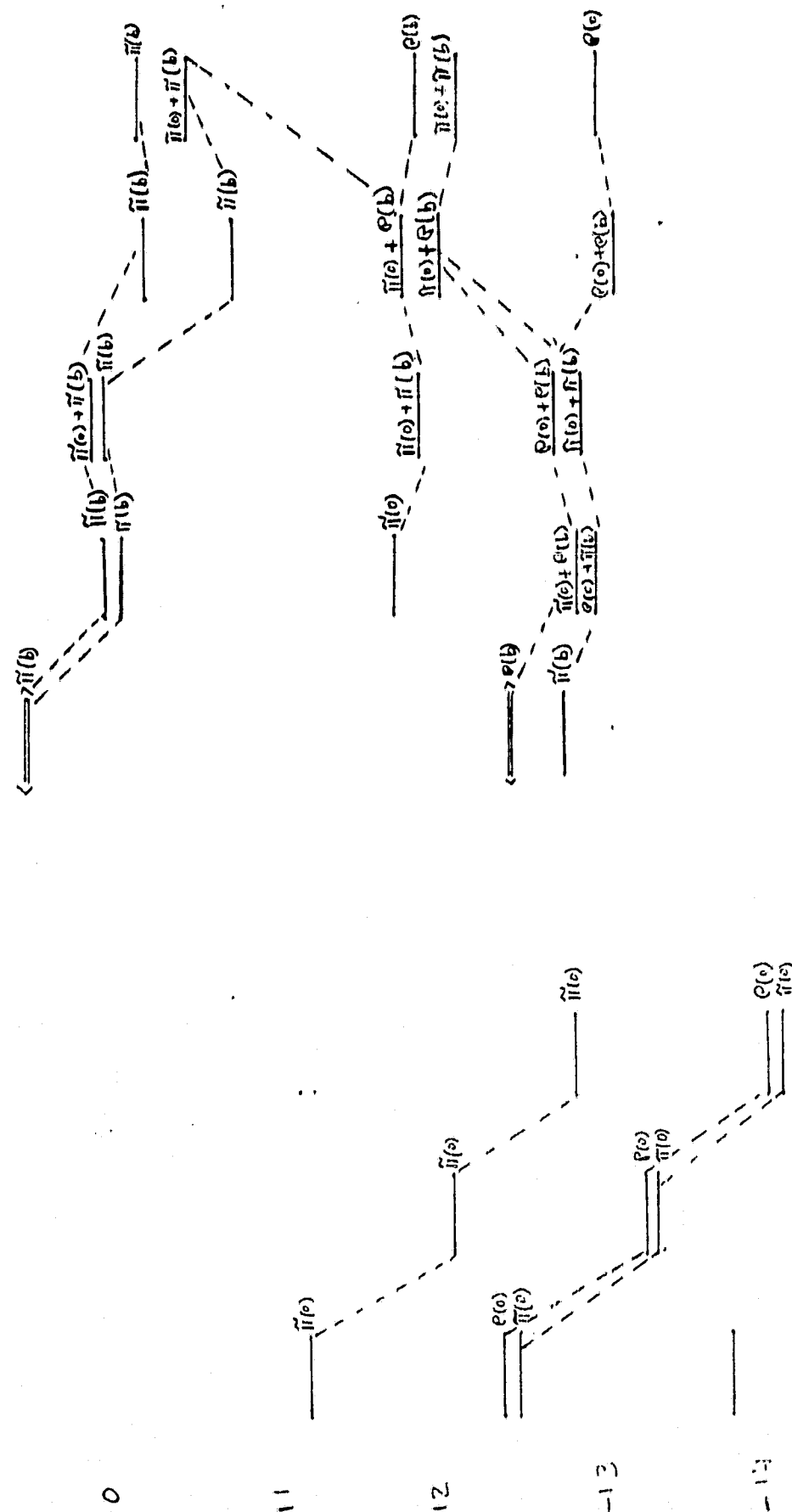


Figure III
 No correlation diagram. Energies are in eV



ORIGINAL PAGE IS
 OF POOR QUALITY

Bimonthly Technical Progress Report I
for the period
October 1, 1981 to November 30, 1981

"Quantum Chemical Calculations for
Polymers and Organic Compounds"

I. Tetracyanoplatinate Compounds

The SCF-X α -DSW relativistic calculations for Pt(CN) $_4^{2-}$ that we completed previously were performed with the following maximum l -value for partial-wave expansion at each center: Outer sphere, $l_{\max} = 4$; Pt, $l_{\max} = 3$; C and N, $l_{\max} = 2$. A non-relativistic calculation with an identical basis set was undertaken in order to establish a detailed comparison with the relativistic results. This calculation was performed also with the SCF-X α -DSW method, but setting the speed of light to infinity. The results should be identical to those obtained using the SCF-X α -SW (Schroedinger) method. However, the molecular orbital energies resulting from this non-relativistic calculation are significantly different from those obtained by Interrante and Messmer in a previous SCF-X α -SW calculation.¹ There are two fundamental differences between our calculation and that of Interrante and Messmer: (1) they used a smaller basis set (outer sphere, $l_{\max} = 3$; Pt, $l_{\max} = 2$; C and N, $l_{\max} = 1$); (2) in our calculation the orbitals 5s and 5p on Pt are considered as core states, whereas Interrante and Messmer include these among the valence states. Consequently, we have a total of 48 valence electrons instead of 56. In order to have an indication of the magnitude of the ligand field shift and splitting of the 5s and 5p orbitals of Pt, we performed an energy search for them by using the last converged potential obtained for our non-relativistic calculation of Pt(CN) $_4^{2-}$. We include also in this search the 4f states since they are even higher in energy than the 5s orbital. In all cases the splittings and shifts were negligible. Thus, we feel that the consideration of 5s, 5p and 4f as core states would not produce any significant change in the SCF energy of the molecular orbitals. In order to understand the importance of the size of the basis set we performed a non-relativistic ($c \rightarrow \infty$) SCF-X α -DSW calculation with identical l_{\max} values than those used by Interrante and Messmer (however, we kept only 48 valence electrons). The molecular orbital energies are only slightly different from those obtained in the non-relativistic calculation with the extended basis. The difference with Messmer calculation is still significant. Thus, in order to ascertain the proper convergence of the DSW results to the Schroedinger SW ones, we performed a calculation with the latter. The results obtained are identical to those of DSW with $c \rightarrow \infty$. We think that the error in the Interrante and Messmer calculation could come from three different sources: (1) computer precision, (2) convergence criterion, (3) since overlapping interatomic spheres are considered, negative intersphere normalization might be present in their calculation.

Finally, a relativistic SCF-X α -DSW calculation with a basis set of intermediate size was also performed. In this calculation l_{\max} of outer sphere was 4, l_{\max} of Pt was 3, and l_{\max} of C and N was 1. Molecular orbital energy diagrams for all the calculations already described are shown in figures 1 and 2. The heading of each column has the following meaning: Messmer 56 corresponds to the Interrante and Messmer calculation; Schro48 is a SCF-X α -SW (Schroedinger) calculation with the reduced basis set; NRDirac48 is a non-relativistic SCF-X α -DSW calculation with the reduced basis set; NRDiPoFn48 is a non-relativistic SCF-X α -DSW calculation with the extended basis set; ReDiPoFn48 is a relativistic SCF-X α -DSW calculation with the extended basis set; and 04Pt3CN1 is a relativistic SCF-X α -DSW calculation with the basis set of intermediate size.

Pt(CN)₄ (-2) MONOMER

figure 1

ENERGY - RYDBERGS

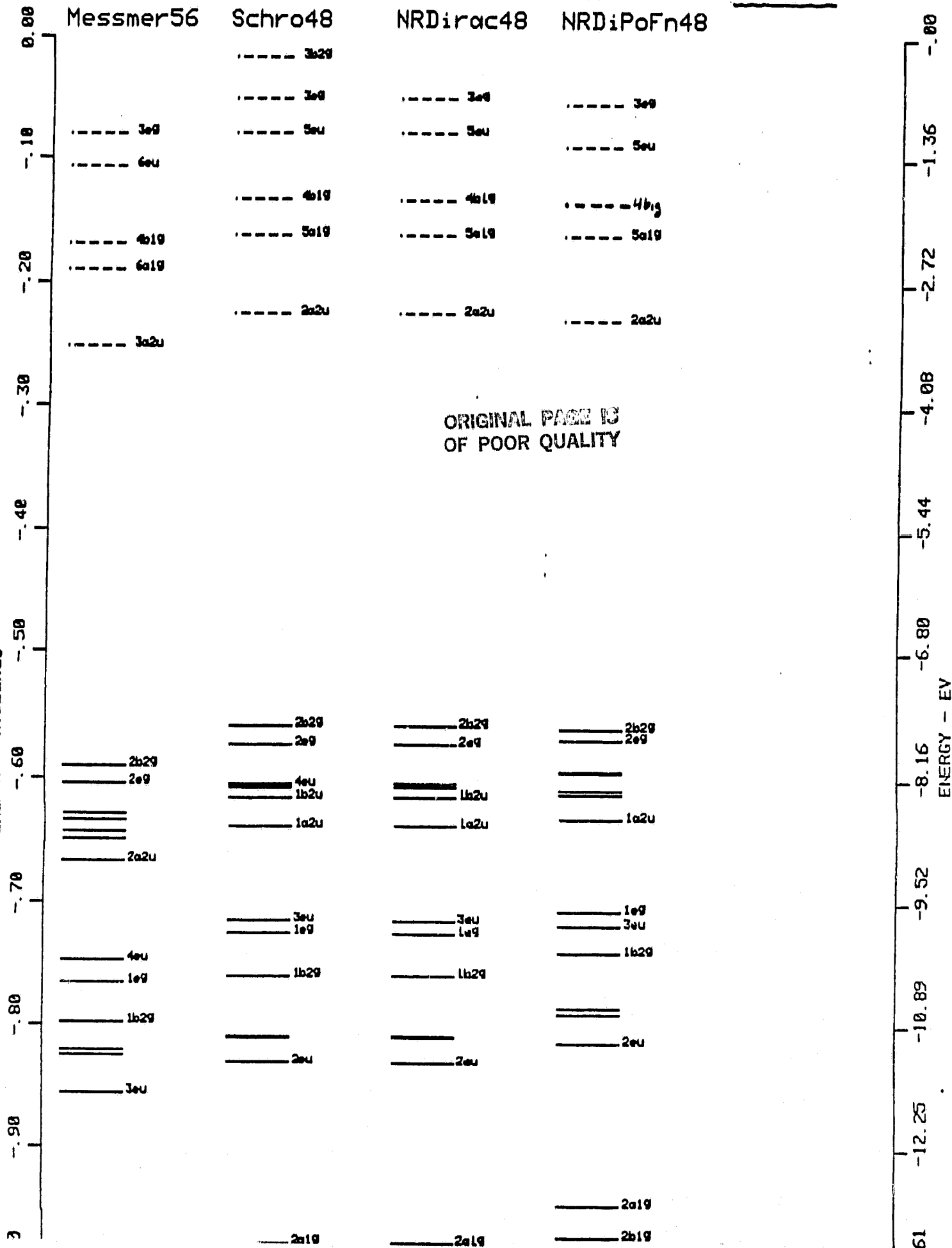
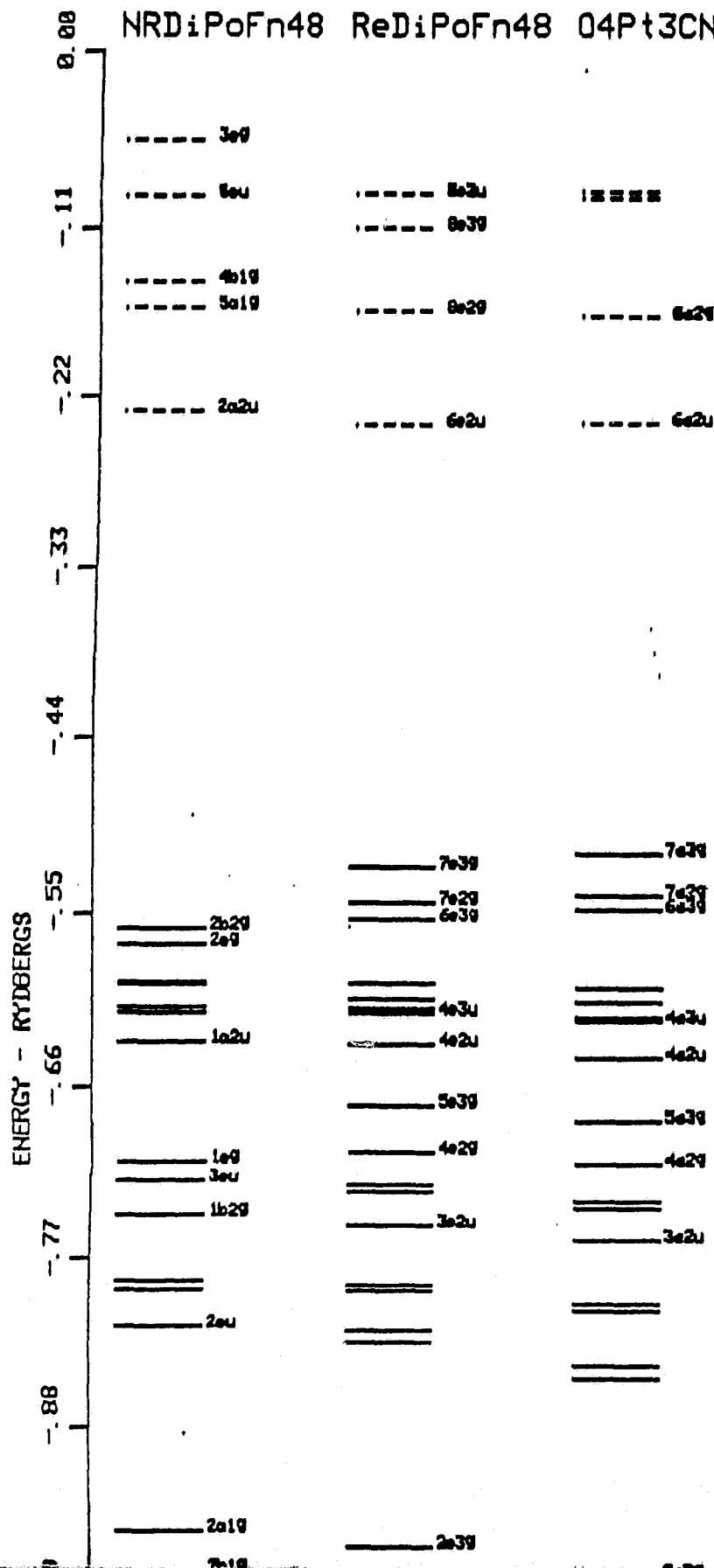


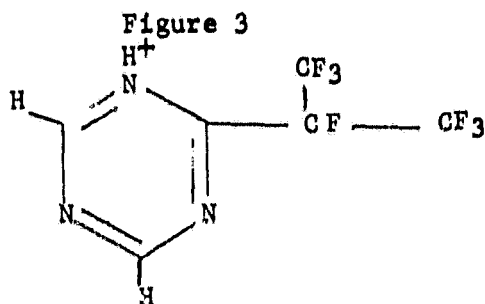
figure 2

NRDiPoFn48 ReDiPoFn48 04Pt3CN1



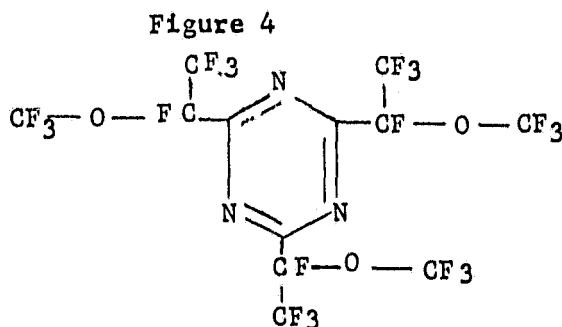
II. Fluoroether Compounds

A MNDO calculation for the protonated specie shown in figure 3 has been completed. The convergence was very slow: complete optimization was obtained after 95 SCF calculations. The protonation appears to be a highly endothermic process, with a protonation enthalpy of the order of 200 kcal/mole. Addition



of a proton produces significant changes in the geometry of the triazing ring; the bond distances as well as the bond angles are modified. The molecular orbital energies are all smaller compared with the unprotonated structure; a manifestation of this is the increase in the ionization potential from 12.3 to 17.2 eV.

The version of the MNDO program that we have been using until now can handle a maximum of 75 basis orbitals. We have been working in modifying the code with the aim to study systems of larger molecular size. Recently we have succeeded in this task: molecular systems with up to 160 basis orbitals (only valence electrons are considered) can now be considered. We have tested the program with the molecule shown in figure 4 which contains a total of 156 orbitals.



We know positively that the iterative process is working correctly; we have been able to perform one calculation with 99 iterations; nevertheless self-consistency has not yet been achieved. The CPU time used in this calculation was about 5 hours (in a VAX machine). We have incremented the number of iterations but for some unknown reason the execution is sometimes interrupted or the output file is empty. Thus, clearly there is a problem with the computer system that we are

using. This machine is very slow, and when the elapsed time is too large (for a CPU time of 5 hours the elapsed time was 17 hours) there are inconsistencies in the response of the system. These facts are suggesting that MNDO calculations for large systems in a VAX computer are becoming to be very impractical. Thus, we are planning to transfer our modified MNDO program to the CRAY 1 computer which should be able to handle these systems more efficiently.

References

- (1) L.V. Interrante and R.P. Messmer, Chem. Phys. Lett. 26, 225(1974)

Bimonthly Technical Progress Report II
for the period
November 23, 1981 to January 22, 1982

"Quantum Chemical Calculations for
Polymers and Organic Compounds"

I. Tetracyanoplatinate Compounds

Both relativistic and non-relativistic calculations on the monomer have shown that the ~~highest occupied molecular orbital (HOMO)~~ has significant contributions from d-like orbitals: 37% (d_{xy} component) for non-relativistic and 57% for relativistic. In both cases there is an orbital that is mostly platinum d_{z^2} -like. This orbital is 0.48 eV and 1.13 eV below the HOMO for the relativistic and non-relativistic calculations respectively. The d_{z^2} character also appears in some other orbitals for both kinds of calculations. ~~is about 1.5 eV below the HOMO. The total amount of d_{z^2} population is about 10%.~~

~~SC~~ ~~Results with two different Pt-Pt distances have been obtained:~~
~~(b)~~
The basis set used in these two calculations corresponds to the one that we called of "intermediate size" in the previous report, that is 244 for the outer sphere, 243 for Pt atoms, and 251 for C and N atoms. Energy level diagrams for these two distances are shown in figure 2. The relativistic energy levels of the monomer (obtained with an equivalent basis set) have also been added to figure 2 for comparison purposes. For the calculation at a Pt-Pt distance of 3.5 Å we found that the HOMO has 42% Pt character. Most of this charge is on the central Pt, having an important contribution from d orbitals in the plane of the ligands. The orbital with the most d_{z^2} character (49% at the central atom and 5% at each peripheral Pt atoms) appears 1.28 eV below the HOMO. When the Pt-Pt distance is shortened to 2.89 Å, the HOMO has now a greater amount of d_{z^2} character: 57.5% (30.1% from central Pt and 13.7% from each peripheral atom). In addition, this HOMO is much more localized on Pt atoms than the HOMO at the larger distance: 85% (at 2.89 Å) vs 42% (at 3.5 Å). The d_{z^2} character is also present in some other orbitals for both distances. Its partial contribution to each MO can be easily seen in figure 3 where the d_{z^2} partial density of states of the central Pt atom is shown for each separation for a wide range of energies. These results so far are pointing towards the following preliminary scenario on

the relationship between partial oxidation and conduction mechanism. The oxidizing agent (the halogen) is removing electrons from planes parallel to the Pt-Pt chain; subsequent shortening of the Pt-Pt distance produces a rearrangement of the orbitals which results in the partial occupation of a d_{z^2} -like energy band. This partially filled band would be responsible for conduction along the Pt-Pt chain. We also performed calculations where 0.9 electrons (in effect creating an oxidation state of +2.3 for each Pt atom) were removed from the d_{z^2} like HOMO. In this case the HOMO still consists of mostly d_{z^2} character, but the d_{z^2} partial density of state shows a significant decrease at the top of the valence band. Extensive analysis of these results are ongoing, and will be presented in the next progress report.

The results obtained for the monomer and trimer will be presented at the March meeting of the American Physical Society to be held in Dallas, Texas.

II. Fluoroether Compounds

A manuscript entitled "MNDO Calculations Applied to Structural Changes in 1,2,4-oxadiazole Substituents", is being sent to Journal of Molecular Structure for publication.

References

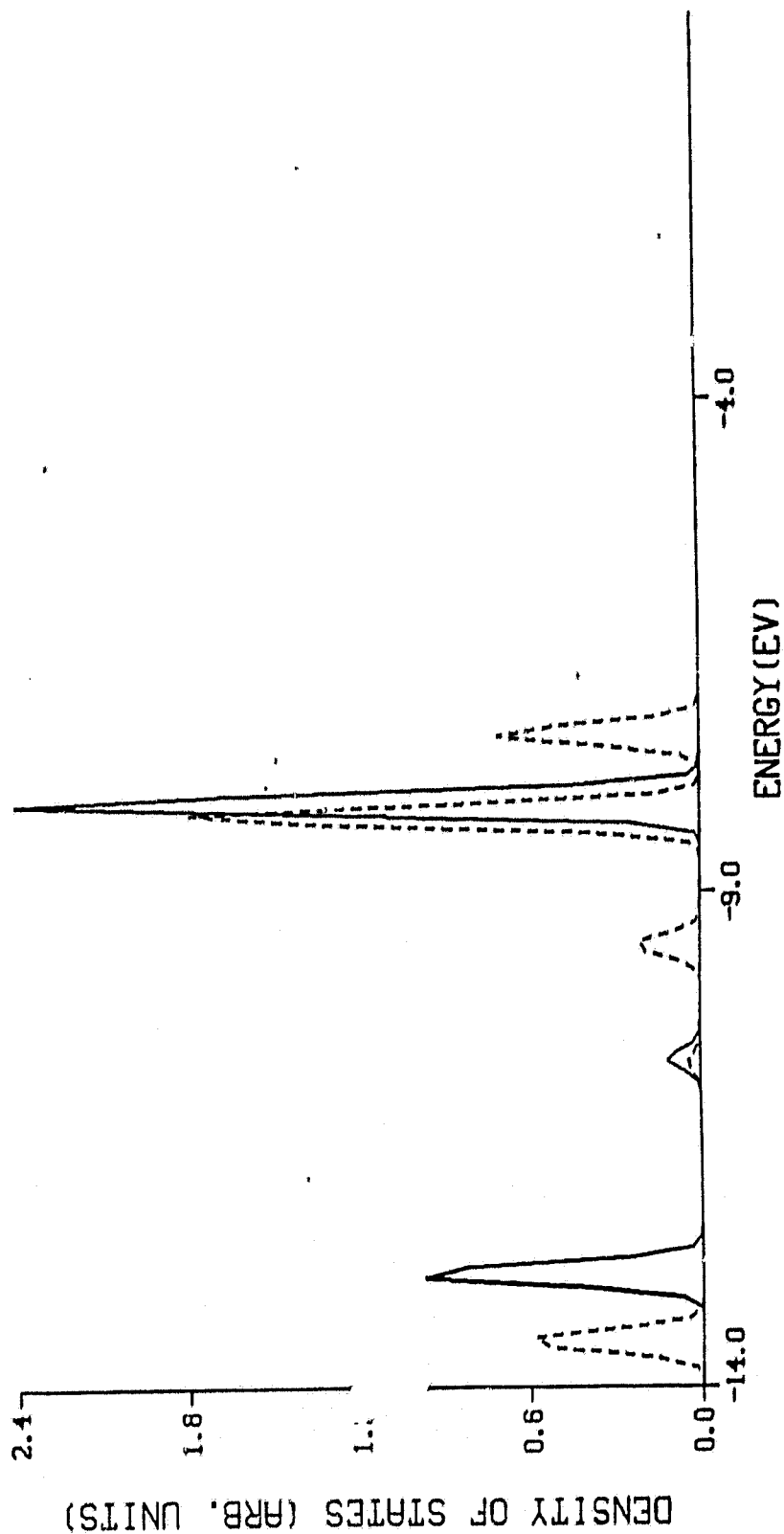
1. M.L. Moreau-Colin, Bull. Soc. Roy. Sci. Liege, 34, 778 (1965).
2. C. Peters and C.F. Eagen, Phys. Rev. Lett. 34, 1132 (1975).
3. J.M. Williams, J.L. Petersen, H.M. Gerdes, and S.W. Peterson, Phys. Rev. Lett. 33, 1079 (1974).

ORIGINAL PAGE IS
OF POOR QUALITY

Figure 1 : $\text{Pt}(\text{CN})_4^{2-}$

SIGMA = 0.10000 MONOMER PARTIAL DZ2 DOS

solid curve : Non-Relativistic
dashed curve : Relativistic



TRIMER VS. MONOMER MONOMER

Figure 2

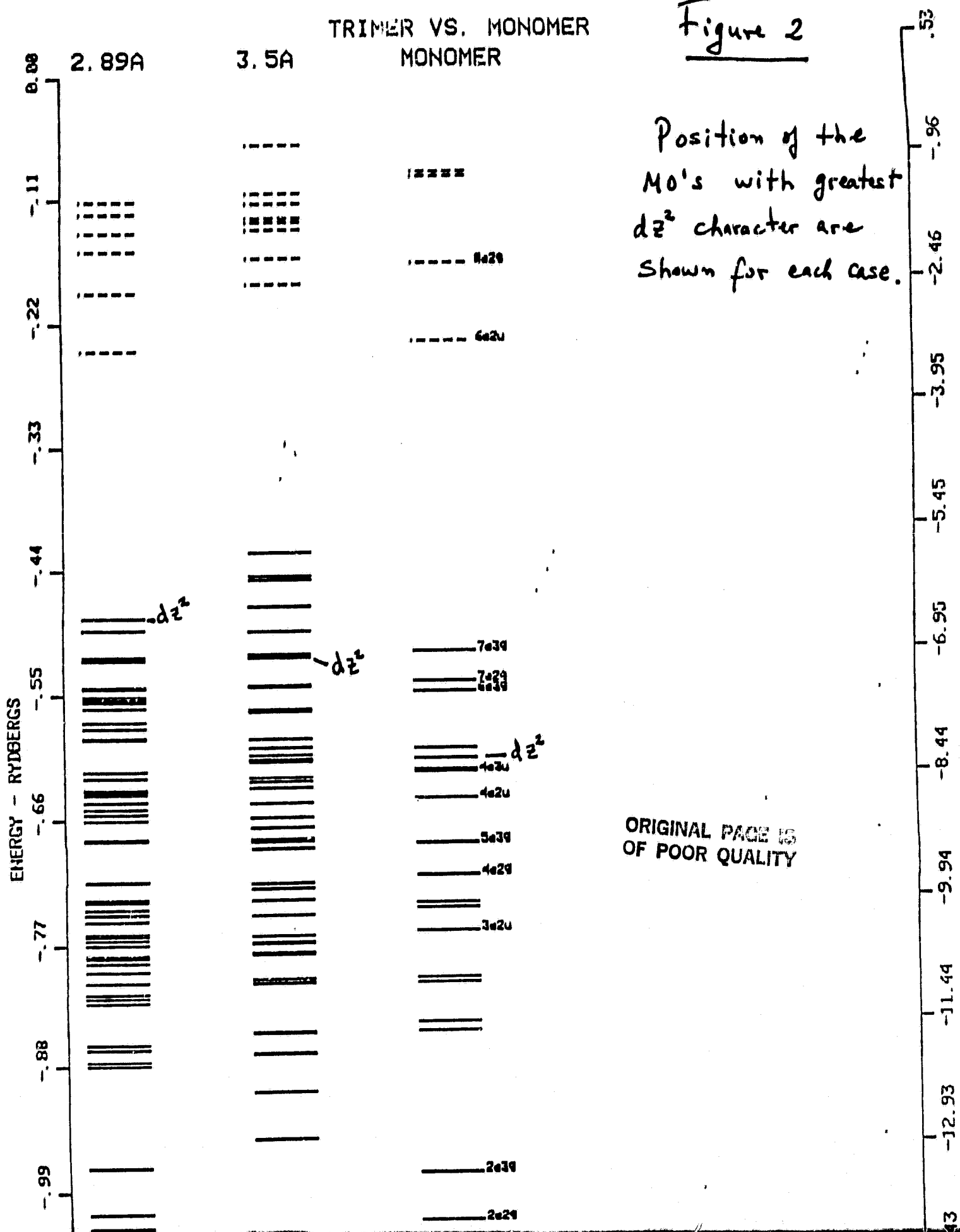


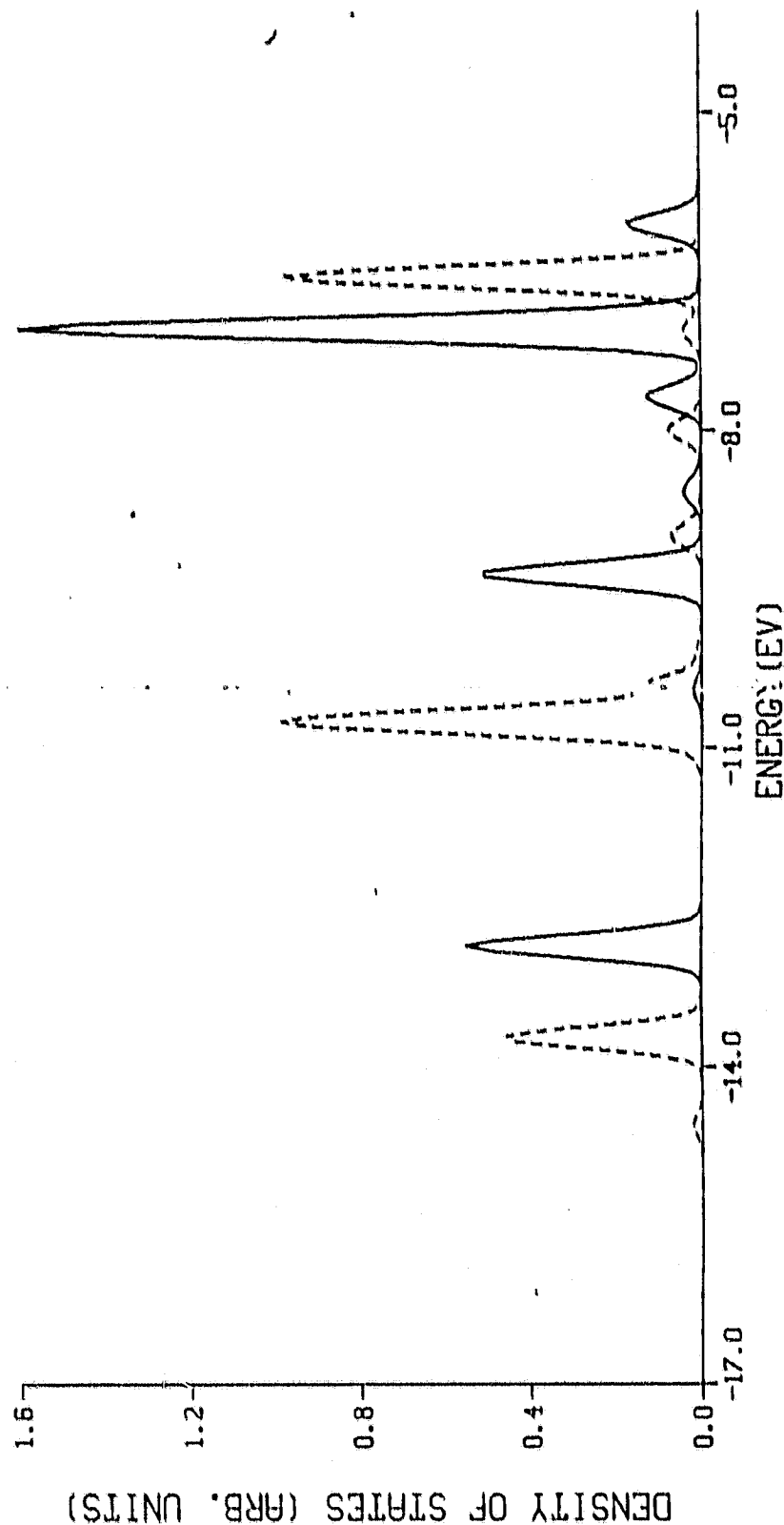
Figure 3 : $[\text{Pt}(\text{CN})_4]_3$ (cluster)

SIGMA = 0.10000

PARTIAL DZ2 3.5A VS 2.89A (Pt-Pt)

Solid curve : 3.5 Å (KISTINE)

dashed curve : 2.89 Å (BR
LOPEZ)



ORIGINAL PAGE IS
OF POOR QUALITY

ORIGINAL PAGE IS
OF POOR QUALITY

Bimonthly Technical Progress Report III
for the period
January 23, 1982 to March 22, 1982

"Quantum Chemical Calculations for
Polymers and Organic Compounds"

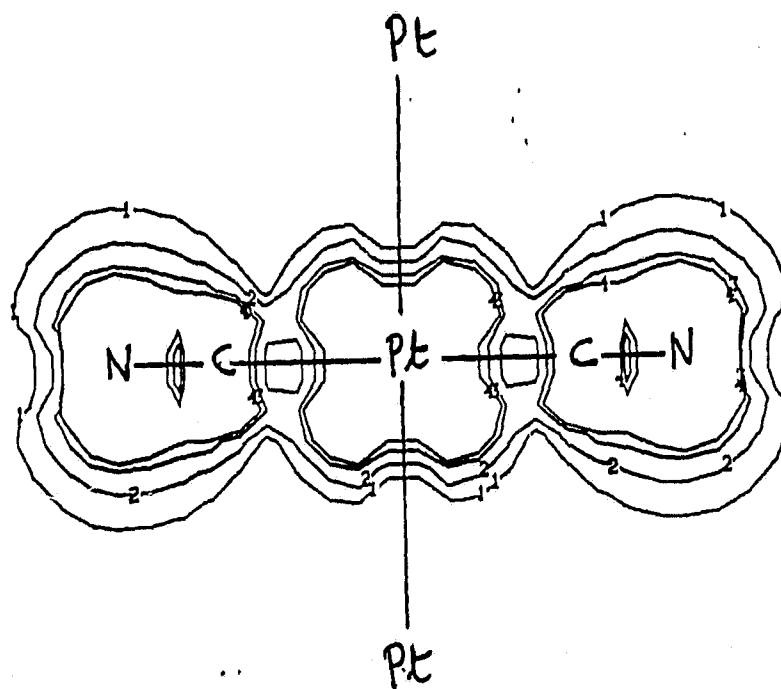
The results of several calculations for the trimer $[\text{Pt}(\text{CN})_4]_3^{-2+q}$ have been extensively analyzed, and a suitable mechanism of the insulator-conductor transition has been formulated. These results were presented during the meeting of the American Physical Society, Dallas, Texas, 8-12 March. In addition, we are in the process of preparing a manuscript to be sent for publication within a few weeks. The findings are summarized below.

The oxidizing dopant removes electrons from a $(d_{\sigma} + d_{\pi})$ -like orbital of the insulator, generating an unstable partially oxidized structure. This structure is stabilized by a process which results in a decrease of the inter-stack distance, accompanied by the energy level reordering of the d_{z^2} and $(d_{\sigma} + d_{\pi})$ orbitals and partial occupation of the d_{z^2} -like orbital. Figure 1 shows a contour map of the electron density of the $(d_{\sigma} + d_{\pi})$ orbital in the plane of the 3 Pt atoms and 2 CN groups of the central $[\text{Pt}(\text{CN})_4]^{2-}$ unit of the cluster. Fig. 2 is a similar contour map, but for the d_{z^2} -like orbital.

The HOMO in the trimer with the insulator inter-stack separation is essentially a non-bonding orbital that is 99.5% localized in the central unit. Since there are no evidences of "surface states" as a result of the cluster model, this orbital probably represents the true nature of the valence band edge in the extended chain. Partial oxidation or removal of nq electrons from this band will create a heterogeneous distribution of charges along the $[\text{Pt}(\text{CN})_4]$ units. This decrease in negative charges of half of the $[\text{Pt}(\text{CN})_4]$ units must in turn produce a decrease in the inter-stack Coulomb repulsion and consequently a shortening of the inter-stack distance. Hence, the antibonding d_{z^2} -like orbital will be pushed up in energy, becoming the new valence band edge. At the same time that the energy crossing of these orbitals is taking place, homogenization of the charge distribution is occurring. The excess of positive charge (in relative terms) generated every other unit due to the removal of electrons from the completely localized $(d_{\sigma} + d_{\pi})$ MO's is returned to the delocalized d_{z^2} -like orbital. This condition is met by transfer of nq electrons from the d_{z^2} -like to the $(d_{\sigma} + d_{\pi})$ -like band. The resulting valence band is partially filled, the charge of each stack being $-2 + q$. Two competing factors resulting from the partial oxidation of the d_{z^2} -band are principally responsible for maintaining the equilibrium prescribed above. Since the d_{z^2} valence band is antibonding between neighboring Pt atoms, its partial oxidation results in a strengthening of the Pt-Pt bond. However, further bond-length contraction is prevented by the net positive charge q created around each Pt atom.

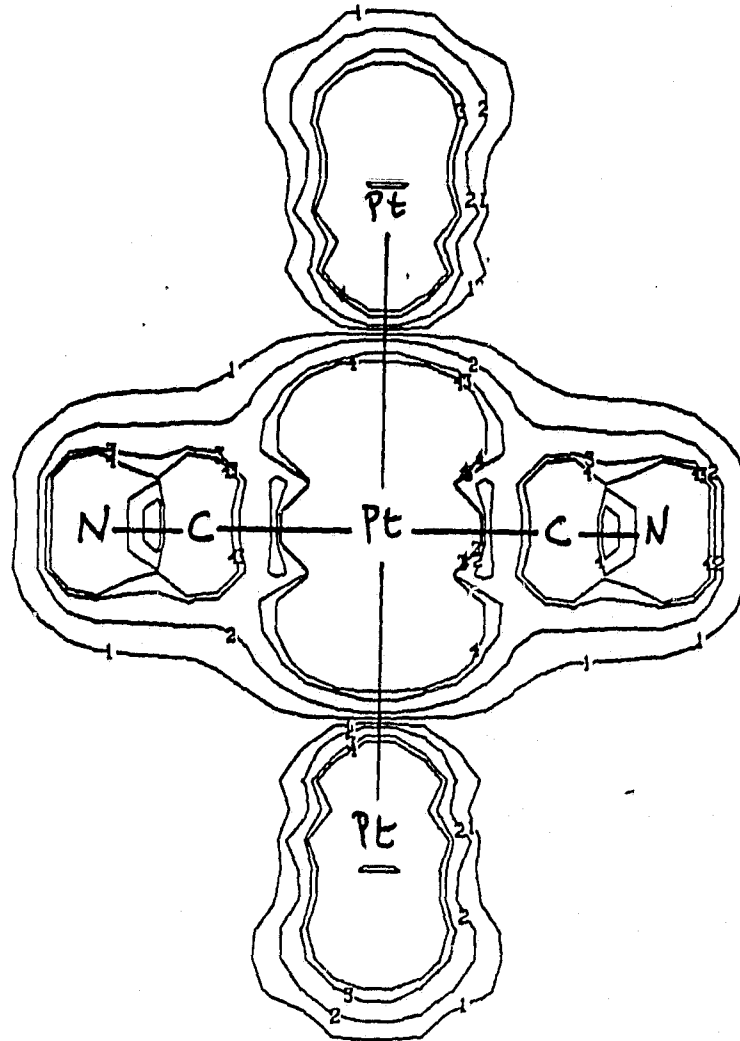
ORIGINAL PAGE IS
OF POOR QUALITY

Figure 1



ORIGINAL PAGE 13
OF POOR QUALITY

Figure 2



Monthly Technical Progress Report
for the period
March 23, 1982 to April 22, 1982

"Quantum Chemical Calculations for
Polymers and Organic Compounds"

A first draft of a manuscript reporting the phenomenon of transition from insulator to conductor in tetracyanoplatinate complexes was finalized during this period. This paper deals principally with the characteristics of the highest occupied molecular orbitals (HOMO) because of their key role in the partial oxidation process. Concurrently we have started examining the charge densities originated from MO's located at energies below the HOMO. Of special interest is the local bonding along the Pt backbone. The charge densities for the trimer $[\text{Pt}(\text{CN})_4]_3$ at a Pt-Pt separation of 3.5 Å have been obtained for several MO's. The results for three of these MO's are shown in Figures 1 to 3. In all cases the contours are expressed in electrons bohrs⁻³. Their values are: 0.00001 (0), 0.00005 (1), 0.00025 (2), 0.00100 (3), 0.00200 (4), and 0.00500 (5). The orbital shown in Figure 1 (with an eigenvalue of -0.686 Rydbergs) is d_{z^2} -like, and has bonding character between Pt atoms. Figures 2 and 3 correspond to charge densities of $(d_\sigma + d_\pi)$ -like orbitals with eigenvalues -0.541 and -0.563 Rydbergs respectively. These orbitals have charges localized on the peripheral $\text{Pt}(\text{CN})_4$ units, and consequently do not contribute to bonding between stacks. All the other MO's studied to date contribute very little to bonding between $\text{Pt}(\text{CN})_4$ units. Analyses of the remaining orbitals are ongoing.

SCF-X α -DSW calculations leading to the interpretation of photo-absorption spectra of aqueous solution of $\text{Pt}(\text{CN})_4$ [1] have been initiated. In these calculations we make use of the transition state concept introduced by Slater [2] in which the relaxation effects of the orbital energies produced by electron excitation are taken into consideration. Our calculations are useful in this study since relativistic effects have been taken into account fully within the one-electron local exchange framework. Comparisons with previous nonrelativistic work by Interrante and Messmer [3] are being made and will be summarized in the next progress report.

Consultation with Dr. M. Golub is continuing on quantum chemical computations. The principal approach used by Dr. Golub is the semi-empirical MNDO molecular orbital method. In conjunction with Dr. Golub, discussion of MNDO results on dichloroethyl ether and sulfide have been ongoing.

REFERENCES

- [1] S.B. Piepho, P.N. Schatz, and A.J. McCaffery, J. Amer. Chem. Soc. 91, 5994 (1969).
- [2] J.C. Slater, "Quantum Theory of Molecules and Solids," McGraw-Hill, New York, Vol. 4, 1974.
- [3] L.V. Interrante and R.P. Messmer, Chem. Phys. Lett. 26, 225 (1974).

ORIGINAL PAGE IS
OF POOR QUALITY

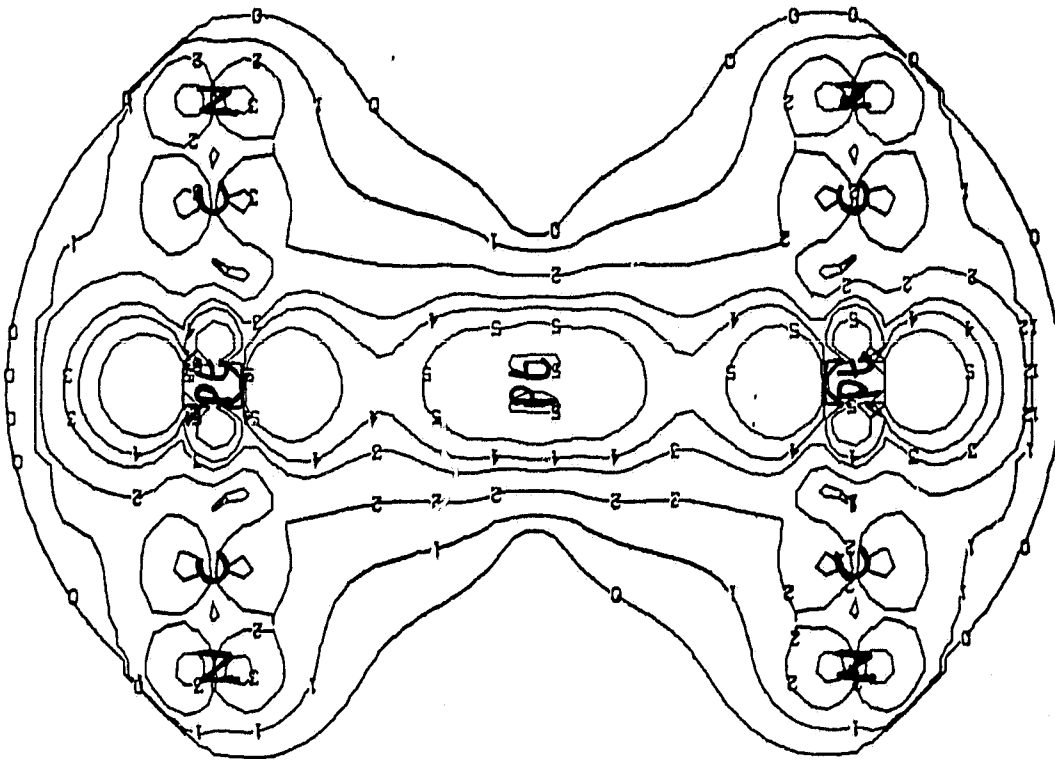


Fig. 1

ORIGINAL PAGE IS
OF POOR QUALITY

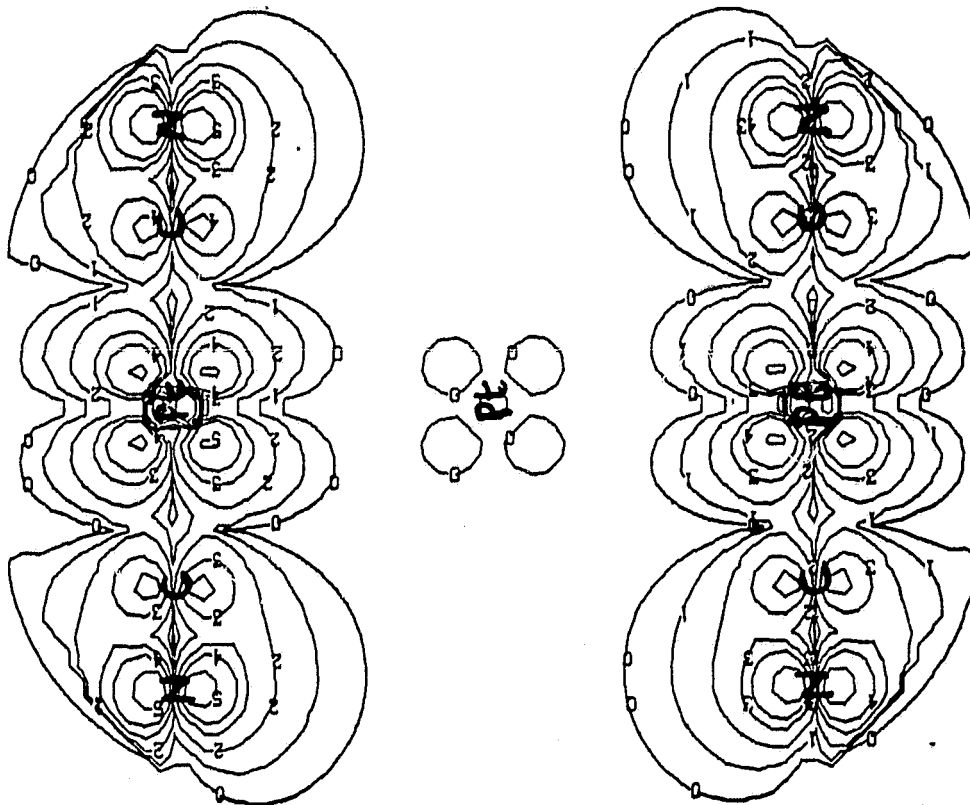


Fig. 2

Fig. 3

ORIGINAL FIGURE
OF POOR QUALITY

